Published in final edited form as:

Cancer Res. 2016 June 1; 76(11): 3295–3306. doi:10.1158/0008-5472.CAN-15-2197.

AMPK activation and metabolic reprogramming by tamoxifen through estrogen receptor-independent mechanisms suggests new uses for this therapeutic modality in cancer treatment

Natalie A. Daurio[1], **Stephen W. Tuttle**[1], **Andrew J. Worth**[2], **Ethan Y. Song**[1], **Julianne M. Davis**[3], **Nathaniel W. Snyder**[4], **Ian A. Blair**[2], and **Constantinos Koumenis**[1]

[1]Department of Radiation Oncology, University of Pennsylvania, Philadelphia PA 19104 USA

[2]Department of Pharmacology, University of Pennsylvania, Philadelphia PA 19104 USA

[3]SUPERS program, University of Pennsylvania, Philadelphia PA 19104 USA

[4]A.J. Drexel Autism Institute, Drexel University, Philadelphia PA 19104 USA

Abstract

Tamoxifen is the most widely used adjuvant chemotherapeutic for the treatment of estrogen receptor (ER) positive breast cancer, yet a large body of clinical and preclinical data indicates that tamoxifen can modulate multiple cellular processes independently of ER status. Here, we describe the ER-independent effects of tamoxifen on tumor metabolism. Using combined pharmacological and genetic knockout approaches, we demonstrate that tamoxifen inhibits oxygen consumption via inhibition of mitochondrial complex I, resulting in an increase in the AMP/ATP ratio and activation of the AMPK signaling pathway *in vitro* and *in vivo*. AMPK in turn promotes glycolysis, and alters fatty acid metabolism. We also show that tamoxifen-induced cytotoxicity is modulated by isoform-specific effects of AMPK signaling, in which AMPKα1 promotes cell death through inhibition of the mTOR pathway and translation. By using agents which concurrently target distinct adaptive responses to tamoxifen-mediated metabolic reprogramming, we demonstrate increased cytotoxicity through synergistic therapeutic approaches. Our results demonstrate novel metabolic perturbations by tamoxifen in tumor cells which can be exploited to expand the therapeutic potential of tamoxifen treatment beyond ER_+ breast cancer.

Keywords

tamoxifen; AMPK; oxidative phosphorylation; synergy; glycolysis

Introduction

Tamoxifen is the most widely used non-steroidal selective estrogen receptor modulator (SERM) for adjuvant therapy of estrogen receptor-positive (ER^+) breast cancer (BC).

Corresponding Author: Constantinos Koumenis, Smilow Center for Translational Research, Room 8-124, Univ. of Pennsylvania, Perelman School of Medicine, 3400 Civic Center Blvd., Bldg 421, Philadelphia, PA 19104-5156, Phone: 215-898-0076, ; Email: costas.koumenis@uphs.upenn.edu

Conflict of Interest: The authors declare no conflict of interest related to this research

Patients on standard treatment receive tamoxifen at 20 mg/day for 5 years during, or shortly after surgical removal of the primary tumor and treatment with ionizing radiation or cytotoxic chemotherapy. Tamoxifen therapy has reduced disease recurrence by half and overall mortality by one-third in ER^+ BC patients. However, the development of tamoxifen resistance remains a significant clinical problem (1,2).

The anti-tumor effects of tamoxifen are attributed primarily to its antiproliferative activity via competitive inhibition of the ER in breast tissue (2). Several studies have previously described non-ER dependent effects of tamoxifen such as the inhibition of Protein Kinase C (PKC)(3) and the sensitization of ER-negative tumors to chemotherapeutic agents (4). Furthermore, during the past two decades, over 25 clinical trials have been published reporting the effects of “high dose” tamoxifen (i.e. doses above those needed to inhibit ER activity) ranging from 80 to 720 mg/day (5) to treat non-breast cancers including glioma (6), melanoma (7) and others (8,9), as a single agent or in combination with chemotherapeutics. While of these Phase I and II trials showed variable clinical benefit, they clearly demonstrated the safety of high dose tamoxifen in diverse patient populations. Pharmacodynamic analyses indicated that tamoxifen could reach plasma concentrations as high as 8μM (8) and additional preclinical studies indicated that tamoxifen accumulates in tumor tissue at 60–70 times the plasma concentration (10). Therefore, further studies on “high dose” tamoxifen are clinically relevant and may result in expanded indications for this affordable and well-tolerated chemotherapeutic.

The chemical properties of tamoxifen as a lipophilic weak base contribute to its high partition into lipid bilayers and tamoxifen has been previously described to have inhibitory effects on mitochondrial respiratory rate (11) and membrane potential (12). Cells in which oxidative phosphorylation (OXPHOS) is inhibited by pharmacologically targeting members of the mitochondrial respiratory chain, or due to lack of oxygen (hypoxia), exhibit a compensatory increase in glycolysis. For example, metformin, a diabetes drug showing promise as a cancer therapeutic, was recently demonstrated to inhibit Mitochondrial complex I and to upregulate glycolysis (13). A defining characteristic of many cancers is the Warburg effect, which denotes an elevated aerobic glycolytic rate, irrespective of any hypoxic burden, as well as an increased dependence on ATP and macromolecule intermediates to support rapid cell growth and division (14). Tumor promotion by certain oncogenes can alter the metabolic characteristics of cells as a requirement for transformation (15). As a result, strategies that target these vulnerable metabolic pathways have shown significant therapeutic promise. For example, both BRAF and KRAS mutations promote glycolysis (16,17). Resistance to targeted therapies limits the therapeutic options in cancers such as melanoma and pancreatic cancer that are driven by these pathways. The drug resistant populations are thus dependent on elevated OXPHOS and drugs that target mitochondrial metabolism, including metformin, have potential utility in targeting such resistant populations (16,18–20).

One of the consequences of OXPHOS inhibition, especially in metabolically active cancer cells, is the activation of the AMP-activated protein kinase (AMPK), the major regulator of cellular energy homeostasis. AMPK is activated when the AMP:ATP ratio increases, signaling a loss in cellular energy charge. AMP binds to the gamma subunit of AMPK

inducing a conformational change that prevents the dephosphorylation of the catalytic alpha subunit of AMPK by phosphatases. This enhances phosphorylation of AMPK by upstream kinases including LKB1 and CaMKK2. Once activated, AMPK restores cellular energy levels by promoting catabolic and inhibiting anabolic processes (21). The role of AMPK in cancer is quite complex as it has been reported to function contextually as both a tumor suppressor or promoter (22).

Based on these studies, we investigated whether tamoxifen had an impact on cellular metabolism and metabolic signaling. Here we report the ability of tamoxifen to inhibit mitochondrial oxygen consumption, increase glycolysis, and alter fatty acid metabolism. We also observe rapid (<10 min) and acute activation of AMPK *in vitro* and *in vivo* in an ER-independent manner. We demonstrate that activation of the AMPK pathway by tamoxifen promotes cell death in triple-negative breast cancer cells in an AMPK-isoform specific manner. Moreover, we demonstrate that cells treated with low μM doses of tamoxifen exhibit increased dependence on glucose metabolism and that pharmacological inhibition of these processes is synergistically lethal with tamoxifen. Overall, this data suggests that tamoxifen functions as a potent regulator of tumor metabolism and AMPK activity and that these metabolic effects can be exploited with combination therapies to increase tumor cytotoxicity.

Materials and Methods

Chemicals and antibodies

Tamoxifen, Fulvestrant, methyl succinate, and spautin-1 were purchased from Sigma Aldrich. The following rabbit polyclonal Antibodies were obtained from Cell Signaling: AMPKα, AMPKα1, phos-AMPKα, phos-ACC, ACC, Phos-p70s6K, phos-s6, phos-4EBP1, cleaved PARP, cleaved caspase 3, and LC3B. ERα antibody purchased from Genetex. AMPKα2 antibody purchased from Millipore. siRNA against PRKAA2 was purchased from Dharmacon.

Cell culture

Cell lines were cultured in Dulbecco's modified eagles medium (DMEM) supplemented with 10% FBS, penicillin/streptomycin, and HEPES at 37°C humidified 5% CO_2 atmosphere. MCF7, MDA-MB-231 and 4175 cell lines were a gift from Andy Minn. LCC1 cells were a gift from Robert Clarke. WM9 and 1205Lu cells were a gift from Meenhard Herlyn (Wistar Institute). Cell lines were authenticated through genetic testing by ATCC.

Oxygen consumption measurements

Oxygen consumption was measured using a YSI 5300a Biological oxygen monitor. Electrodes were equilibrated in media for 10 minutes. Cells were trypsinized and suspended at $2x10^7$ cells per mL and injected into the chamber at a 1:10 dilution. After oxygen consumption rate was recorded, drug was injected into the chambers at 10μM increments, allowing consumption rate to be determined after each injection. Total protein per chamber was quantified by Lowry assay.

Isolation of liver mitochondria

Liver was removed from a sacrificed mouse and homogenized in 8 volumes of sucrose buffer (0.25 M sucrose, 0.02 M KCl, 0.005 M $MgCl_2$, 0.01 M KH_2PO_4 (pH= 7.4). Homogenate was spun at 600 x g for 5 min at 4°C. The supernatant was then transferred to a new tube and centrifugation was repeated. Cleared supernatant was spun at 9000 x g for 10 min at 0°C and the pellet was resuspended in sucrose buffer. The following conditions were used for respiration measurements: Complex 1 respiration: Sucrose buffer + 0.1 mM ADP, 5 mM glutamate and 5 mM malate. Complex 2 respiration: Sucrose buffer + 0.1 mM ADP and 5 mM sodium succinate.

Cell survival assays

see supplemental methods.

Immunoblot analysis

see supplementary methods

Generation of CRISPR-Cas9 knockout cell lines

Knock out cell lines were generated using the CIRSPR-cas9 system as previously described (23). sgRNAs were designed to target the first exon of the genes of interest using the CRISR design tool at http://crispr.mit.edu/. Two sgRNA sequences were chosen for each gene of interest (supplemental table S1). Briefly, sgRNA's were cloned into CRISPR-cas9 plasmid. pSpCas9(BB)-2A-Puro (PX459) was a gift from Feng Zhang (Addgene plasmid # 48139). Cells were transfected using lipofectamine 2000 and carrier DNA. Media was changed 24hrs after transfection and cells were selected with puromycin for 48hrs. Remaining cells grown up and clones were selected. Clones were screened for gene excision or mutation by DNA gel and expression of the protein of interested by western blot. Knock out was successful using both *PRKAA1* sgRNA's 1 and 2. Knock out of *ESR1* expression required combined transfection of sgRNA 1 and 2.

HPLC quantification of AMP and ATP

AMP and ATP quantified using a previously published method (24). Briefly, 2–4x10^6 cells were plated in 10cm^2 dishes and treated with tamoxifen. Cells were then pelleted and nucleotides extracted with perchloric acid. Extracts were analyzed by ion pair reverse phase HPLC. Analysis was carried out on a Jasco HPLC. Separation was performed on SUPELCOSIL C18 column (15 cm x 4.6 mm, 3 μm particle size) in combination with a Supelguard Acentis C18 guard column (2 cm x 4.0 mm) from Sigma.

LC-MS/MS metabolite analysis

Liquid chromatography-selected reaction monitoring (LC-SRM)/MS analysis of acyl-CoA thioesters. Methods were previously described in detail (25). CoAs were separated using a reversed-phase HPLC Phenomenex Luna C18 column (2.0 mm × 150 mm, particle size 3.5 μm) with 5 mM ammonium acetate in water as solvent A, 5 mM ammonium acetate in ACN/water (95:5; v/v) as solvent B, and ACN/water/formic acid (80:20:0.1; v/v/v) as solvent C. Samples were analyzed using an API 4000 triple-quadrupole mass spectrometer (Applied

Biosystems, Foster City, CA) in the positive electrospray (ESI) mode. Samples (10 μL) were injected using a Leap CTC autosampler (CTC Analytics, Switzerland) where they were maintained at 4 °C.

Short-chain and Long-chain acyl-CoA extraction

Extractions were performed as described in detail previously (25), (26). See supplementary methods.

Lactate extraction and analysis by LC-MS/MS

Media was aspirated and cells were quenched by the direct addition of 1 mL −80 °C 4:1 methanol:water (v/v) to the cell culture dish. Plates were placed at −80 °C for 20 min then scraped and transferred into Eppendorf tubes. Samples were pulse sonicated on ice for 30 sec at a rate of 1 pulse/sec prior to centrifugation at 16,000 x *g* at 4 °C for 10 min. The supernatants were then transferred to clean glass tubes and evaporated to dryness under nitrogen. Dried residues were resuspended in 100 μL of mobile phase A for LC-MS analysis. For labeling studies cells were grown in media omitting glucose supplemented with 1 mg/mL [$^{13}C_6$]-glucose. Details of the LC-MS/MS analysis have been describes in detail previously (27). Quantification of tamoxifen and metabolites in tumor tissue: Frozen tissue was weighed and homogenized by electric homogenizer on ice in 4:1 methanol:water (v/v). Samples were then centrifuged at 16,000 x *g* at 4 °C for 10 min. 10 μL of the resulting supernatant was analyzed by reverse phase LC-MS/MS utilizing teniposide as the internal standard for absolute quantification.

siRNA transfection

see supplemental methods.

BODIPY 493/503 staining

BODIPY lipid probes were purchased from Molecular Probes. Staining solution was made up at 2μg/mL in PBS. After drug treatments, cells were fixed using 4% Paraformaldehyde and stored at 4°C. Neutral lipid staining was performed by pelleting the cells and re-suspending in staining solution and incubated for 10mins at room temperature. Cells were washed 2x with PBS, suspended in 500 μL PBS and strained. Cells were analyzed for mean BODIPY stain intensity by flow cytometry (FL1-H).

[^{35}S] labeling

Cells were plated in 60mm dish and treated for experimental conditions. Cells were incubated with methionine/cysteine free media for 30 min. Hot labeling media made up at 0.075mCi/mL [^{35}S]-methionine/cysteine. Cells were incubated with labeling media for 30 mins. Cells were washed with cold PBS and harvested for protein. Protein assay preformed on cold samples and equal amounts of [^{35}S] labeled protein were resolved on sodium dodecyl sulfate polyacrylamide gels. Gel was washed with fixing solution (water with 20% methanol, 10% acetic acid) for 30 min, washed with DI water, then washed with enlightening solution (PerkinElmer) for 30 min. Gel was dried overnight using a BioRad gel

drying apparatus. Gel was exposed to autoradiography film at −80°C and film was developed.

Orthotopic xenograft tumors

Four-week old female nu/nu mice were purchased from Charles River Laboratories and housed in the University of Pennsylvania animal facility maintained on a 12h light/dark cycle and given free access to water and food *ad libitum*. $2x10^6$ 4175 cells suspended in 50 μL of a 50/50 mixture of PBS and Matrigel Matrix basement membrane (Corning) were injected into the mammary fat pad.

In vivo Tamoxifen treatment

Tamoxifen was dissolved 20 mg in 200 μL ethanol and 800 μL peanut oil. Ethanol was evaporated off overnight. Mice were dosed via intraperitoneal injection once per day for 3 days at 100 mg/kg.

Protein analysis from tumors

See supplementary methods.

Statistical analysis

All statistical analyses were performed using a two-tailed Student's t test assuming homoscedasticity. A p value < 0.05 was considered statistically significant.

Results

Tamoxifen inhibits OXPHOS and cellular oxygen consumption independently of ER inhibition

While tamoxifen has been reported to affect mitochondrial electron transport and membrane potential, its effects on oxygen consumption have not been adequately described. A Clark-type electrode was used to measure oxygen consumption of cells. Tamoxifen, at low μM doses, inhibited oxygen consumption in a dose dependent manner in both ER^+ MCF7 cells and triple-negative MDA-MB-231 cells (figure 1A). Tamoxifen also inhibited oxygen consumption in a panel of 6 non-breast cancer cell lines (supplemental table S2). The active metabolite of tamoxifen, 4-hydroxy-tamoxifen (4OH-Tam) also inhibited oxygen consumption while the ER antagonist fulvestrant, which inhibits ER activity by blocking ER dimerization and promoting degradation of the ER (28), did not have a significant effect (Supplemental Figure S1A). This suggests that inhibition of ER signaling is not responsible for the rapid inhibition of oxygen consumption in response to tamoxifen treatment. To further rule out involvement of ER signaling in tamoxifen-mediated inhibition of oxygen consumption, we used the CRISPR-Cas9 system to knock out ERα from LCC1 cells, a variant of the MCF7 line which expresses functional ER but is not dependent on its signaling for proliferation (29). The ability of tamoxifen to inhibit oxygen consumption in the LCC1-crspER cells was no different from the parental LCC1 cells. Moreover, fulvestrant treatment, which leads to downregulation of total ER protein levels, had no impact on the ability of tamoxifen to inhibit oxygen consumption in MCF7 cells (Supplemental Figure S1B), further

supporting the notion that tamoxifen inhibits oxygen consumption independently of ER signaling.

Tamoxifen inhibits oxygen consumption by blocking complex I of the mitochondrial respiratory chain

To determine if the effect of tamoxifen on oxygen consumption was due to a direct interaction with mitochondria, we permeabilized MCF7 and MDA-231 cells using digitonin. Tamoxifen inhibited oxygen consumption of mitochondria by approximately 60% in both permeabilized cell lines. Respiration could be rescued by supplementation with electron transport chain complex II substrate succinate but not with complex I substrates, glutamate and malate (figure 1D). These effects of tamoxifen on mitochondria respiration are similar to what is seen with rotenone, a known complex I inhibitor (figure 1D). In mitochondria isolated from mouse liver, tamoxifen also inhibited oxygen consumption in the presence of glutamate and malate but not in the presence of succinate (supplemental figure S1C). This indicates that the tamoxifen-mediated inhibition of oxygen consumption occurs through a direct effect on mitochondria, upstream of complex II. The addition of methyl succinate, a cell-permeable analog of succinate, to media, reduced the ability of tamoxifen to inhibit oxygen consumption in intact BC cells (figure 1E) and significantly increased cell survival of MCF7 cells treated with tamoxifen (figure 1F). These results suggest that inhibition of mitochondrial function upstream of complex II, mediates the effects of tamoxifen on oxygen consumption and downstream effects.

Tamoxifen rapidly activates AMPK and AMPK-dependent signaling

To determine if inhibition of oxygen consumption by tamoxifen alters cellular energy charge we quantified intracellular AMP and ATP pools following tamoxifen treatment. Tamoxifen increased the AMP:ATP ratio in MDA-231 cells and MCF7 cells (figure 2A) the major activating mechanism of AMPK, as soon as 5 min after tamoxifen treatment and this ratio further increased following one hour of treatment. This increase in the AMP:ATP ratio correlated with concomitant increase in tamoxifen- induced AMPK phosphorylation of the downstream signaling target acetyl-CoA carboxylase (ACC) and dephosphorylation of the mTOR targets P70S6K, S6 and 4EBP1, in both MCF7 (figure 2B) and MDA-MB-231 cells (figure 2C). To investigate if ER signaling is necessary for tamoxifen activation of the AMPK pathway, we used pharmacologic and genetic methods to block ER signaling. Pretreatment with fulvestrant did not inhibit tamoxifen activation of AMPK (figure 2D). Furthermore, activation of AMPK in LCC1-crspER was comparable to that in LCC1 parental cells (figure 2E), indicating that the effects of tamoxifen on AMPK signaling are also ER-independent.

Tamoxifen treatment increases glycolysis

AMPK activation is known to increase glycolytic activity in an attempt to restore cellular ATP pools (21). To investigate if this occurred following tamoxifen treatment, we measured glucose uptake from the media in MDA-231 and MCF7 cells. Glucose uptake increased in a dose-dependent manner with tamoxifen treatment in both cell lines (figure 3A). To examine if glycolysis was also upregulated by tamoxifen we analyzed the incorporation of [^{13}C] from [^{13}C]6-Glucose into acetyl-CoA and lactate by LC-MS/MS. Following tamoxifen treatment

we observed an increase in [^{13}C] labeling in these products, indicating an increase in glycolytic activity (figure 3B and 3C). The activation of AMPK (P-AMPK) was enhanced under glucose deprivation conditions (figure 3D) and treatment with the glycolytic inhibitor 2-deoxyglucose (2DG) (supplemental figure S1E) in both MCF7 and MDA-231 cells, underscoring the importance of the glycolytic switch for ATP generation during tamoxifen treatment. Interestingly, under glucose deprivation conditions, supplementation with methyl succinate rescues MDA-231 cells from tamoxifen treatment whereas it does not significantly improve MDA-231 survival in complete media (supplemental figure S1D). This effect further highlights the importance of glycolysis during tamoxifen treatment.

Tamoxifen impacts fatty acid metabolism

Products of glucose metabolism are used for synthesis of fatty acids (FAs) which are of particular importance in cancer due to the need to generate excess membranes for rapid proliferation. Moreover, the oxidation of FAs in the mitochondria can replenish cellular ATP levels during times of metabolic stress (30). To examine if tamoxifen also impacted FA metabolism, we preformed metabolite analysis of Fatty acyl-CoA species by LC-MS/MS. This analysis showed an accumulation of acetyl-CoA and malonyl-CoA following tamoxifen treatment (Supplemental Figure S2A). We also observed a reduction in succinyl-CoA and other medium chain acyl-CoA species (C3:0, C6:0) consistent with reports of the effects of other complex I inhibitors (31) and an accumulation of longer chain (C16-C20) acyl-CoA species (Supplemental Figure S2A). The addition of [^{13}C]-glucose or [^{13}C]-glutamine resulted in no labeling of the long-chain CoA metabolites, indicating that these fatty acyl-CoAs are not synthesized from glucose or glutamine *de novo* in response to tamoxifen treatment. Activation of the AMPK pathway is also known to promote β-oxidation of fatty acids as a strategy to increase ATP pools. The degradation of lipid droplets by autophagy, termed lipophagy, increases the supply of free FAs which are then transported into the mitochondria for oxidation (30). We also observed a rapid activation of autophagy upon tamoxifen treatment (Figure 3E). BODIPY stain, which measures total neutral lipid content in the cell, decreased modestly after 4 hours of tamoxifen treatment, by 14%, in cells treated with tamoxifen (Supplemental Figure S2B and S2C). These data suggest that the accumulation of the long chain acyl-CoA species results from breakdown of lipid droplets.

AMPK isoforms differentially regulate survival in response to tamoxifen treatment

To further dissect the biological role of AMPK in the cellular response to tamoxifen, we used the CRISPR-cas9 system to knock out AMPKα1. We observed that loss of AMPKα1 resulted in a compensatory increase in AMPKα2 expression (Figure 4A) and had increased survival in response to tamoxifen treatment (figure 4C). This effect was recapitulated in MCF7 cells where AMPKα1 inhibition by shRNA resulted in reduced levels of cleaved PARP and increased survival upon tamoxifen treatment compared to shNT-transfected cells (supplemental figure S3A and S3B). To evaluate the impact of complete inhibition of AMPK catalytic activity on cellular response to tamoxifen, we used siRNA to knock down AMPKα2 in both wild type MDA-231 cells and in crspAMPKα1 cells. Loss of AMPKα2 in MDA-231 cells resulted in increased cell death upon tamoxifen treatment (figure 4C) whereas knockdown of AMPKα2 in the AMPKα1 CRISPR knockout cells resulted in further increase in tamoxifen-induced cytotoxicity.

Interestingly, knockdown of either isoform of AMPKα resulted in loss of phospho-ACC upon tamoxifen treatment, while loss of AMPKα1 alone ameliorated the inhibition of the mTOR pathway following tamoxifen treatment. Induction of autophagy remained unchanged upon AMPKα1 inhibition; however, knockdown of both isoforms substantially reduced autophagy levels as seen by a reduction in LC3 processing (figure 4A). To further investigate the role of AMPK isoforms in the autophagic response of BC cells to tamoxifen treatment we pretreated cells with E64d and pepstatin A to prevent LC3-II recycling and monitored autophagic flux by immunoblot. While we saw reduced levels of LC3 in both siAMPKα2 and crspAMPKα1 conditions, MDA-231 cells require both AMPKα1 and AMPKα2 to be knocked down in order to significantly reduce autophagy induction with tamoxifen treatment (Figure 4B). This data suggests that AMPK activation promotes autophagy in response to tamoxifen treatment. To determine if the AMPK isoform-specific effects on the mTOR pathway impacted upon cellular translation, we pulse-labeled MDA-231 cells and crspAMPKα1 cells with [^{35}S]-cysteine and methionine. Translation was inhibited in both cell lines, albeit to a substantially lesser extent in the crspAMPKα1 cells upon tamoxifen treatment (Figure 4D and Supplemental Figure S3E).

Notably, while the dual AMPKα1/2 knockdown showed the highest levels tamoxifen toxicity as determined by modified MTT assay, the levels of apoptosis markers cleaved PARP and cleaved Caspase 3 were quite low. This could be due to more rapid processing of these markers under these conditions as indicated by complete loss of total PARP in these cells. Caspase 3/7 activity assay suggests a decrease in apoptosis upon AMPKα1 knock out while Annexin V and propidium iodide staining support an increase in apoptosis with AMPKα2 knock down (supplemental figure S3C). However, the data from these apoptosis assays were not statistically significant and showed only a small trend towards different levels of apoptosis dependent on AMPK status. Crystal violet staining of cells 7 days following tamoxifen treatment, also shows that AMPKα1 knock out rescues cells from tamoxifen treatment while AMPKα2 knock down promotes cell death (supplemental figure S3D). Therefore, although increased apoptosis may contribute to reduced viability of AMPKα2 knockout cells following tamoxifen treatment, additional mechanisms leading to reduced overall survival are likely involved.

Tamoxifen activates the AMPK pathway in an orthotropic model of breast cancer

To determine if tamoxifen activates the AMPK pathway *in vivo,* we injected 4175 cells, a variant of the MDA-MB-231 triple negative breast cancer cell line (32) into the mammary fat pad of athymic nude female mice. After 3 weeks of tumor growth, 100mg/kg tamoxifen was administered once daily for 3 days. Mean tamoxifen and metabolite levels of 4-hydroxy-tamoxifen and N-desmethyl-tamoxifen quantified by LC-MS/MS in the tumor tissue were 19.07, 3.97 and 33.64 ng/mg respectively (figure 5A). This data indicates that the concentrations of tamoxifen needed to activate the AMPK pathway *in vitro* are achievable *in vivo*. Mice treated with tamoxifen also had significantly higher levels of phospho-AMPK and displayed downregulation of the mTOR target phospho-4-EBP1 (figure 5B and figure 5C). These results are in agreement with AMPK pathway activation seen *in vitro*.

Synergistic combination of tamoxifen and inhibitors of glycolysis increases cytotoxicity

Dual blockade of required metabolic pathways to target tumor cells is gaining significant traction in preclinical and clinical settings. In terms of metabolic targeting, it has been postulated that concurrently targeting adaptive responses to metabolic reprogramming can lead to significant enhancement of the therapeutic window for multiple chemotherapeutic modalities (33,34). Since we demonstrated that tamoxifen blocks OXPHOS and concurrently increases glucose uptake and utilization, it is likely that effective strategies for metabolic targeted therapies may require the inhibition of both OXPHOS and glycolysis simultaneously. 2DG, a non-metabolizable analog of glucose and 3-Bromopyruvate (3BP), an alkylating agent and inhibitor of hexokinase-2 and glyceraldehyde 3-phosphate dehydrogenase (GAPDH), induced a dose-dependent decrease in glucose uptake, as expected (Figure 6A and 6C). More importantly, combined treatment with relatively non-toxic doses of each of these inhibitors (supplemental Figure S1F), with tamoxifen significantly enhanced tamoxifen-induced cytotoxicity in MCF7 cells and in MDA-231 cells (Figures 6B and 6D). Notably, the sensitization to tamoxifen was larger in the MDA-231 cells, which display a higher basal rate of glucose uptake (Figure 3A) and lower basal OXPHOS level (Figure 1B).

Discussion

We have demonstrated that beyond its anti-estrogenic effects, tamoxifen exerts a pronounced effect on tumor metabolism via a non-ER, mitochondrial-specific pathway. Specifically, through the inhibition of oxygen consumption upstream of complex II, the increase in AMP/ATP ratio leads to activation of AMPK, enhancement of glycolytic activity, and loss of neutral lipid stores. We also discovered a previously unreported dichotomy in the role of AMPK isoforms in tumor survival following metabolic stress. Whereas AMPKα1 primarily appears to promote cell death through inhibition of the mTOR pathway and translation, AMPKα2 promotes survival by a yet unidentified mechanism. We have also identified a strategy in which these metabolic perturbations induced by tamoxifen can be exploited for therapeutic benefit through combination therapy with glycolytic inhibitors

While the clinical benefit of tamoxifen in ER^+ breast cancer patients has been mainly attributed to inhibition of ER activity, tamoxifen has previously been shown to have multiple effects independent of ER. We have further characterized the effects of tamoxifen on mitochondria by describing the dose dependent effects on oxygen consumption to occur independent of ER. We have also demonstrated that AMPK activation occurs in both ER^+ and ER^- BC cells and that it is independent of ER signaling. In addition, tamoxifen activated the AMPK pathway in an orthotopic model of triple negative breast cancer. While we treated these animals for a short time at a high dose, we would anticipate similar effects at a lower dose over a longer period of time, as tamoxifen has been shown to accumulate in tumor tissues to levels up to 60–70 times the plasma concentration (10).

The non-ER dependent effects of tamoxifen described here, have the potential to expand the therapeutic window for tamoxifen into ER− BC and non-breast cancers. Furthermore, most ER+ BC related deaths have been attributed to metastatic disease which is often tamoxifen-resistant (2). While the mechanism by which tamoxifen resistance occurs remains unclear, it

is thought to involve alterations in ER itself and alterations in the levels of co-regulators or downstream effectors in the signaling pathway (2). Our results suggest that it would be valuable to further explore whether combination therapies that take advantage of the metabolic effects of tamoxifen could restore tamoxifen sensitivity or prevent resistance.

The precise target for tamoxifen in the mitochondrial respiration chain is not currently clear. The evidence presented in this manuscript supports the hypothesis that tamoxifen inhibits complex I in the electron transport chain (see Figure 7). The ability of complex II substrate succinate to restore oxygen consumption in tamoxifen treated cells points to the inhibition of mitochondrial respiration upstream of complex II. Moreover, the inability of complex I substrates glutamate and malate to restore any oxygen consumption in permeabilized BC cells indicates that complex I may be the site of tamoxifen action (Figure 7). However, we cannot completely rule out possible effects of tamoxifen on upstream processes, such as the TCA cycle, that contribute electron donors to the respiratory chain. Another implication of our findings with translational potential is the fact that inhibition of oxygen consumption is a validated strategy to increase tumor pO2 and decrease hypoxia, a major cause of cancer resistance to genotoxic therapy, including radiation (35). Therefore, tamoxifen has the potential to function as a radiation and chemotherapeutic sensitizer. In fact, other complex I inhibitors, such as metformin, have shown anti-cancer effects through both their metabolic effects and activation of AMPK. Although our results are reminiscent of the metabolic effects of metformin treatment, both the inhibition of oxygen consumption and activation of AMPK occur at a far more rapid rate (5–10 mins) than that seen with metformin (12–24hrs). Also important is the distinction that while *in vitro* metformin exerts its OXPHOS-inhibitory effects at doses ranging from 1–50 mM, tamoxifen does so at low μM concentrations.

We also show that like metformin, tamoxifen inhibited OXPHOS and increased dependence on glycolysis (Figure 7). Intriguingly, soon after BC patients begin treatment with tamoxifen, a “metabolic flare” is often seen in their FDG-PET scans (36). Although the cause for this radiologic abnormality has not been clearly delineated, it is reasonable to hypothesize that this could be due to increased uptake of FDG in response to metabolic reprogramming and AMPK activation, since GLUT 1 transporters, the major transporter system of glucose and FDG uptake, are AMPK targets (37).

Our results are also in agreement with other metabolic effects of tamoxifen in patient populations. Women on tamoxifen therapy have an increased risk for developing non-alcoholic fatty liver disease (38). However, the effects of tamoxifen on tumor fatty acid metabolism have not been investigated in detail. Accumulation of malonyl-CoA following tamoxifen treatment has been previously reported (39) and we also observed this in BC cells. The synthesis of malonyl-CoA is the rate-limiting step in fatty acid synthesis, thus its accumulation leads us to suspect that there is a decrease in the activity of FASN which is consistent with AMPK activation. It is also possible that increased upstream flux through glycolysis, contributes to the accumulation of malonyl-CoA with tamoxifen treatment. It is worth noting that AMPK is also known to inhibit fatty acid synthesis and promote β-oxidation, primarily through inhibiting ACC (21).

The anti-tumorigenic effects of metformin in BC have been shown to be dependent on its activation of AMPK (40). We asked if AMPK had a similar role in BC survival of tamoxifen treatment. We used the CRISPR-cas9 system to delete AMPKα1 from MDA-MB-231 cells and observed a compensatory increase in AMPKα2 expression. This would lead us to hypothesize that the isoforms have redundant effects, yet, we observed opposing effects on cell survival. Other work examining the isoforms of AMPKα has identified some differences, including the suppression of α2 expression in primary BC (41). Knock out of AMPKα1 alone rescued cells from tamoxifen treatment while knock down of AMPKα2 increased cell death. Immunoblot analysis and [^{35}S] labeling of proteins indicated that the α1 subunit is responsible for downregulation of the MTOR pathway and translation. However, both isoforms are needed to inhibit ACC and either isoform can activate autophagy. We suspect that it is the loss of robust autophagy induction in the dual AMPKα1α2 knockdown that results in increased tamoxifen cytotoxicity under those conditions. The ability of tamoxifen to activate autophagy is well established. In fact, the autophagic response to tamoxifen as been implicated in BC resistance to tamoxifen treatment (42,43). In addition, the ability of AMPK to activate autophagy via ULK1 is also well described (44). The data reported in this manuscript is the first to directly identify AMPK activation as a mechanism of autophagy induction in tamoxifen treatment. In summary, we have identified AMPK as a mediator of tamoxifen toxicity through isoform specific effects.

We have also demonstrated the potential for increased therapeutic benefit through drug combinations with tamoxifen that have a synergistic effect via blockade of upregulated metabolic pathways. Due to the fact that inhibition of oxygen consumption by tamoxifen results in upregulated glycolysis, effective strategies for metabolic interventions may require the inhibition of both OXPHOS and glycolysis simultaneously. Glycolytic inhibitors have long been attractive clinical agents due to the Warburg effect, yet systemic toxicity has limited their success in the clinic. 2DG has been tested in clinical trials and 3BP has shown significant preclinical potential (45). Our data suggests that clinical use of these inhibitors in combination with tamoxifen may result in increased efficacy and use of reduced doses that may limit toxicity.

In conclusion, we have characterized the ER-independent effects of tamoxifen on cancer metabolism and described how these effects can be exploited for therapeutic benefit through novel drug combinations with the potential to expand the clinical use of tamoxifen.

Supplementary Material

Refer to Web version on PubMed Central for supplementary material.

Acknowledgments

We acknowledge the support of NIH grants 2R25CA140116-06, P30CA016520, P30ES013508, and T32ES019851.

References

1. EBCTCG. Effects of chemotherapy and hormonal therapy for early breast cancer on recurrence and 15-year survival: an overview of the randomised trials. Lancet. 2005; 365:1687–717. [PubMed: 15894097]
2. Osborne CK. Tamoxifen in the treatment of breast cancer. N Engl J Med. 1998; 339:1609–18. [PubMed: 9828250]
3. O'Brian CA, Liskamp RM, Solomon DH, Weinstein IB. Inhibition of protein kinase C by tamoxifen. Cancer Res. 1985; 45:2462–5. [PubMed: 3157445]
4. McClay EF, Albright KD, Jones Ja, Christen RD, Howell SB. Tamoxifen modulation of cisplatin sensitivity in human malignant melanoma cells. Cancer Res. 1993; 53:1571–6. [PubMed: 8453625]
5. Stuart NS, Philip P, Harris aL, Tonkin K, Houlbrook S, Kirk J, et al. High-dose tamoxifen as an enhancer of etoposide cytotoxicity. Clinical effects and in vitro assessment in p-glycoprotein expressing cell lines. Br J Cancer. 1992; 66:833–9. [PubMed: 1358168]
6. Tang, Pa; Roldan, G.; Brasher, PMa; Fulton, D.; Roa, W.; Murtha, a, et al. A phase II study of carboplatin and chronic high-dose tamoxifen in patients with recurrent malignant glioma. J Neurooncol. 2006; 78:311–6. [PubMed: 16710748]
7. McClay EF, McClay ME, Jones Ja, Winski PJ, Christen RD, Howell SB, et al. A phase I and pharmacokinetic study of high dose tamoxifen and weekly cisplatin in patients with metastatic melanoma. Cancer. 1997; 79:1037–43. [PubMed: 9041168]
8. Perez, Ea; Gandara, DR.; Edelman, MJ.; O'Donnell, R.; Lauder, IJ.; DeGregorio, M. Phase I trial of high-dose tamoxifen in combination with cisplatin in patients with lung cancer and other advanced malignancies. Cancer Invest. 2003; 21:1–6. [PubMed: 12643003]
9. Bergan RC, Reed E, Myers CE, Headlee D, Brawley O, Cho HK, et al. A Phase II study of high-dose tamoxifen in patients with hormone-refractory prostate cancer. Clin cancer Res. 1999; 5:2366–73. [PubMed: 10499606]
10. Lien, Ea; Solheim, E.; Ueland, PM. Distribution of tamoxifen and its metabolites in rat and human tissues during steady-state treatment. Cancer Res. 1991; 51:4837–44. [PubMed: 1893376]
11. Moreira PI, Custódio J, Moreno A, Oliveira CR, Santos MS. Tamoxifen and estradiol interact with the flavin mononucleotide site of complex I leading to mitochondrial failure. J Biol Chem. 2006; 281:10143–52. [PubMed: 16410252]
12. Cardoso CMP, Moreno AJM, Almeida LM, Custódio JBa. 4-Hydroxytamoxifen induces slight uncoupling of mitochondrial oxidative phosphorylation system in relation to the deleterious effects of tamoxifen. Toxicology. 2002; 179:221–32. [PubMed: 12270594]
13. Wheaton WW, Weinberg SE, Hamanaka RB, Soberanes S, Sullivan LB, Anso E, et al. Metformin inhibits mitochondrial complex I of cancer cells to reduce tumorigenesis. Elife. 2014; 2014:1–18.
14. Vander Heiden MG, Cantley LC, Thompson CB. Understanding the Warburg effect: the metabolic requirements of cell proliferation. Science (80-). 2009; 324:1029–33.
15. Boroughs LK, DeBerardinis RJ. Metabolic pathways promoting cancer cell survival and growth. Nat Cell Biol Nature Publishing Group. 2015; 17:351–9.
16. Ying H, Kimmelman AC, Lyssiotis Ca, Hua S, Chu GC, Fletcher-Sananikone E, et al. Oncogenic kras maintains pancreatic tumors through regulation of anabolic glucose metabolism. Cell Elsevier Inc. 2012; 149:656–70.
17. Haq R, Fisher DE, Widlund HR. Molecular pathways: BRAF induces bioenergetic adaptation by attenuating oxidative phosphorylation. Clin Cancer Res. 2014; 20:2257–63. [PubMed: 24610826]
18. Haq R, Shoag J, Andreu-Perez P, Yokoyama S, Edelman H, Rowe GC, et al. Oncogenic BRAF regulates oxidative metabolism via PGC1α and MITF. Cancer Cell Elsevier Inc. 2013; 23:302–15.
19. Yuan P, Ito K, Perez-lorenzo R, Del Guzzo C, Lee JH, Shen C-H, et al. Phenformin enhances the therapeutic benefit of BRAF V600E inhibition in melanoma. PNAS. 2013; 110:18226–31. [PubMed: 24145418]
20. Viale A, Pettazzoni P, Lyssiotis Ca, Ying H, Sánchez N, Marchesini M, et al. Oncogene ablation-resistant pancreatic cancer cells depend on mitochondrial function. Nature. 2014; 514:628–32. [PubMed: 25119024]

21. Mihaylova MM, Shaw RJ. The AMPK signalling pathway coordinates cell growth, autophagy and metabolism. Nat Cell Biol Nature Publishing Group. 2011; 13:1016–23.
22. Liang J, Mills GB. AMPK: A contextual oncogene or tumor suppressor? Cancer Res. 2013; 73:2929–35. [PubMed: 23644529]
23. Ran F, Hsu P, Wright J, Agarwala V. Genome engineering using the CRISPR-Cas9 system. Nat Protoc. 2013; 8:2281–308. [PubMed: 24157548]
24. Kochanowski N, Blanchard F, Cacan R, Chirat F, Guedon E, Marc a, et al. Intracellular nucleotide and nucleotide sugar contents of cultured CHO cells determined by a fast, sensitive, and high-resolution ion-pair RP-HPLC. Anal Biochem. 2006; 348:243–51. [PubMed: 16325757]
25. Basu SS, Blair Ia. SILEC: a protocol for generating and using isotopically labeled coenzyme A mass spectrometry standards. Nat Protoc Nature Publishing Group. 2012; 7:1–12.
26. Snyder NW, Basu SS, Zhou Z, Worth AJ, Blair Ia. Stable isotope dilution liquid chromatography/mass spectrometry analysis of cellular and tissue medium- and long-chain acyl-coenzyme A thioesters. Rapid Commun Mass Spectrom. 2014; 28:1840–8. [PubMed: 25559454]
27. Aird KM, Worth AJ, Snyder NW, Lee JV, Sivanand S, Liu Q, et al. ATM couples replication stress and metabolic reprogramming during cellular senescence. Cell Rep The Authors. 2015; 11:893–901.
28. Osborne CK, Wakeling A, Nicholson RI. Fulvestrant: an oestrogen receptor antagonist with a novel mechanism of action. Br J Cancer. 2004; 90:S2–6. [PubMed: 15094757]
29. Brünner N, Boulay V, Fojo A, Freter CE, Lippman ME, Clarke R. Acquisition of hormone-independent growth in MCF-7 cells is accompanied by increased expression of estrogen-regulated genes but without detectable DNA amplifications. Cancer Res. 1993; 53:283–90. [PubMed: 8380254]
30. Rambold AS, Cohen S, Lippincott-Schwartz J. Fatty acid trafficking in starved cells: Regulation by lipid droplet lipolysis, autophagy, and mitochondrial fusion dynamics. Dev Cell Elsevier Inc. 2015; 32:1–15.
31. Worth, aJ; Basu, SS.; Snyder, NW.; Mesaros, C.; Blair, Ia. Inhibition of neuronal cell mitochondrial complex I with rotenone increases lipid -oxidation supporting acetyl-coenzyme A levels. J Biol Chem. 2014; 289:26895–903. [PubMed: 25122772]
32. Minn AJ, Gupta GP, Siegel PM, Bos PD, Shu W, Giri DD, et al. Genes that mediate breast cancer metastasis to lung. Nature. 2005; 436:518–24. [PubMed: 16049480]
33. Dörr JR, Yu Y, Milanovic M, Beuster G, Zasada C, Däbritz JHM, et al. Synthetic lethal metabolic targeting of cellular senescence in cancer therapy. Nature. 2013; 501:421–5. [PubMed: 23945590]
34. Sonveaux P, Végran F, Schroeder T, Wergin MC, Verrax J, Rabbani ZN, et al. Targeting lactate-fueled respiration selectively kills hypoxic tumor cells in mice. J Clin Invest. 2008; 118:3930–42. [PubMed: 19033663]
35. Lin A, Maity A. Molecular pathways: A novel approach to targeting hypoxia and improving radiotherapy efficacy via reduction in oxygen demand. Clin cancer Res. 2015; 21:1995–2000. [PubMed: 25934887]
36. Dehdashti F, Flanagan FL, Mortimer JE, Katzenellenbogen JA, Welch MJ, Siegel BA. Positron emission tomographic assessment of " metabolic flare " to predict response of metastatic breast cancer to antiestrogen therapy. Eur J Nucl Med Mol Imaging. 1999:26.
37. Wu N, Zheng B, Shaywitz A, Dagon Y, Tower C, Bellinger G, et al. AMPK-dependent degradation of TXNIP upon energy stress leads to enhanced glucose uptake via GLUT1. Mol Cell Elsevier Inc. 2013; 49:1167–75.
38. Saphner T, Triest-Robertson S, Li H, Holzman P. The association of nonalcoholic steatohepatitis and tamoxifen in patients with breast cancer. Cancer. 2009; 115:3189–95. [PubMed: 19484789]
39. López M, Lelliott CJ, Tovar S, Kimber W, Gallego R, Virtue S, et al. Tamoxifen-induced anorexia is associated with fatty acid synthase inhibition in the ventromedial nucleus of the hypothalamus and accumulation of malonyl-CoA. Diabetes. 2006; 55:1327–36. [PubMed: 16644689]
40. Zakikhani M, Dowling R, Fantus IG, Sonenberg N, Pollak M. Metformin is an AMP kinase-dependent growth inhibitor for breast cancer cells. Cancer Res. 2006; 66:10269–73. [PubMed: 17062558]

41. Fox MM, Phoenix KN, Kopsiaftis SG, Claffey KP. AMP-activated protein kinase α 2 isoform suppression in primary breast cancer alters AMPK growth control and apoptotic signaling. Genes Cancer. 2013; 4:3–14. [PubMed: 23946867]

42. Samaddar JS, Gaddy VT, Duplantier J, Thandavan SP, Shah M, Smith MJ, et al. A role for macroautophagy in protection against 4-hydroxytamoxifen-induced cell death and the development of antiestrogen resistance. Mol Cancer Ther. 2008; 7:2977–87. [PubMed: 18790778]

43. Cook KL, Shajahan AN, Wärri A, Jin L, Hilakivi-Clarke La, Clarke R. Glucose-regulated protein 78 controls cross-talk between apoptosis and autophagy to determine antiestrogen responsiveness. Cancer Res. 2012; 72:3337–49. [PubMed: 22752300]

44. Kim J, Kundu M, Viollet B, Guan K-L. AMPK and mTOR regulate autophagy through direct phosphorylation of Ulk1. Nat Cell Biol Nature Publishing Group. 2011; 13:132–41.

45. Ko YH, Smith BL, Wang Y, Pomper MG, Rini Da, Torbenson MS, et al. Advanced cancers: Eradication in all cases using 3-bromopyruvate therapy to deplete ATP. Biochem Biophys Res Commun. 2004; 324:269–75. [PubMed: 15465013]

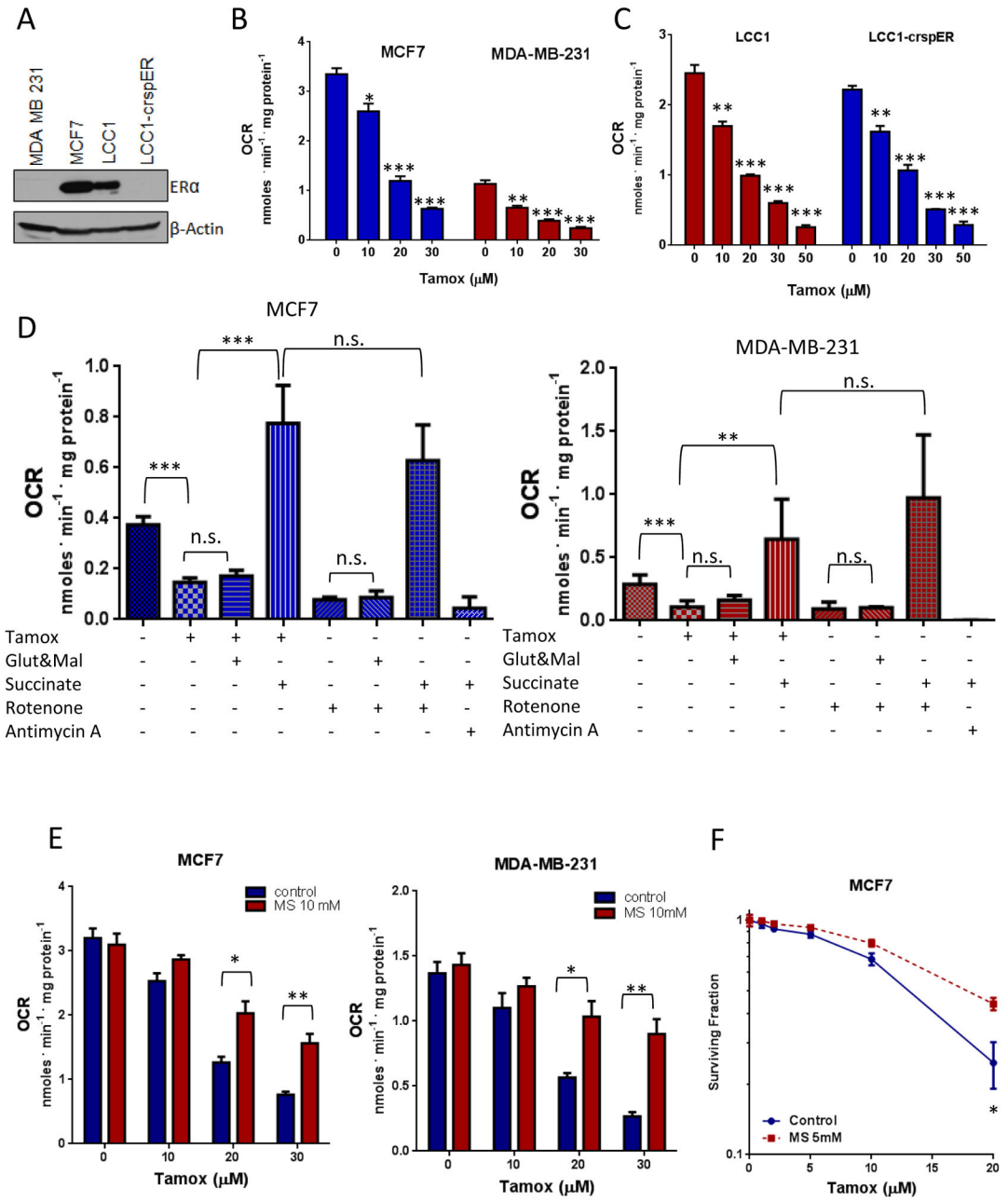

Figure 1. Tamoxifen inhibits cellular OXPHOS in an ER independent manner

A. Immunoblot of ER expression in BC cell lines B. Cellular oxygen consumption measurements in response to increasing doses of tamoxifen in ER+ MCF7 cells and ER- MDA-MB-231 cells. C. Cellular oxygen consumption in LCC1 cells and LCC1 cells with CRISPR-Cas9 mediated deletion of ERα. Data are the average of three independent experiments ±SEM, **P<0.01 ***P<0.001. D. Effect of tamoxifen on oxygen consumption of digitonin permeabilized MDA-231 and MCF7 Cells in the presence of complex I or complex II substrates. Data are the average of three independent experiments ±SEM **P<0.01 ***P<0.001. E. Oxygen consumption in MCF7 and MDA-231 cells treated with

Tamoxifen alone or in the presence of methyl succinate. Data are the average of three independent experiments ±SEM *P<0.05 **P<0.01. F. Survival of MCF7 cells (N=6) treated with tamoxifen alone or in the presence of methyl succinate, ±SEM, *P<0.05.

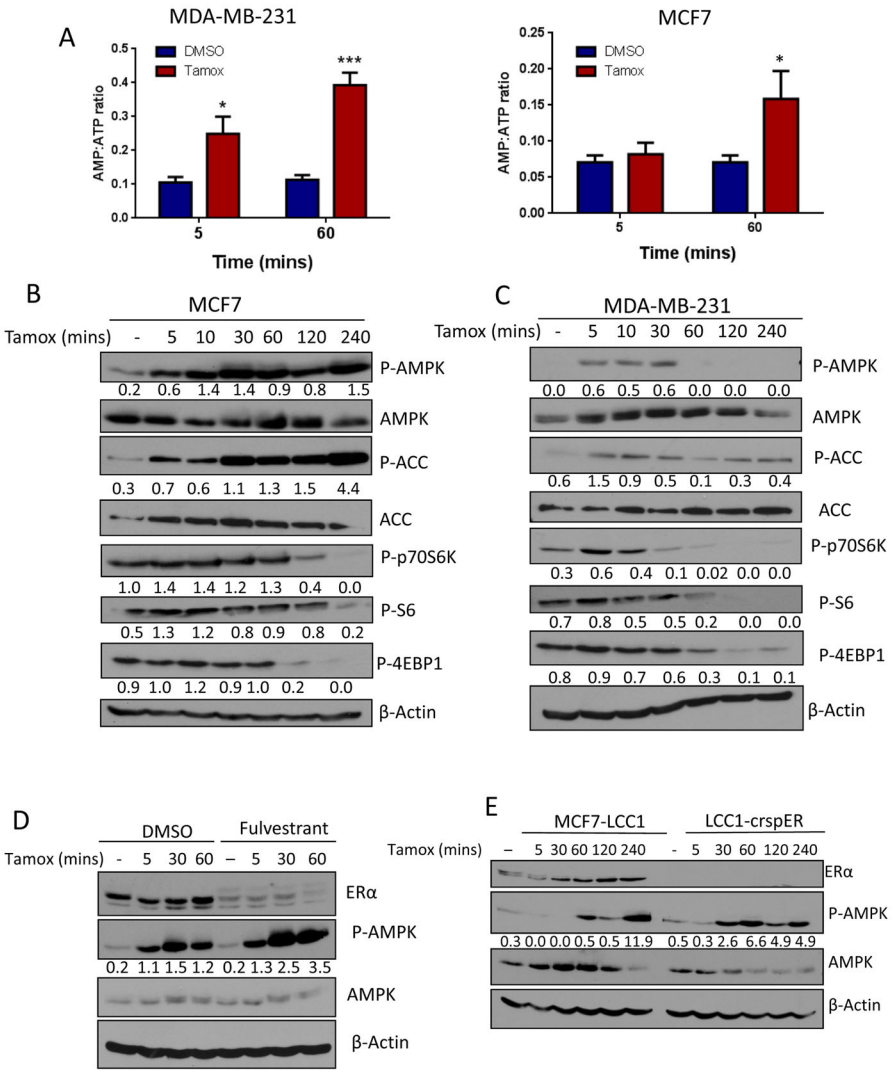

Figure 2. Tamoxifen rapidly and acutely activates AMPK independently of estrogen receptor signaling

A. HPLC quantification of the AMP:ATP ratio in MDA-MB-231 (N=6) and MCF7 (N=3) cells treated with 30μM tamoxifen for 5 and 60 mins, ±SEM *P<0.05 **P<0.01. B. Immunoblot of AMPK pathway activation following treatment with 30μM tamoxifen in MCF7 and C. in MDA-MB-231 cells. D. Immunoblot analysis of ER expression and AMPK activation in MCF7 cells treated with 10μM fulvestrant or DMSO for 4hrs preceding treatment with 30μM tamoxifen over time. E. Immunoblot of AMPK activation in LCC1 cells and LCC1 cells with CRISPR-Cas9 deletion of ERα. Values below blots represent pixel intensity normalized to loading control: P-AMPK/AMPK, P-ACC/ACC, or normalized to β-Actin.

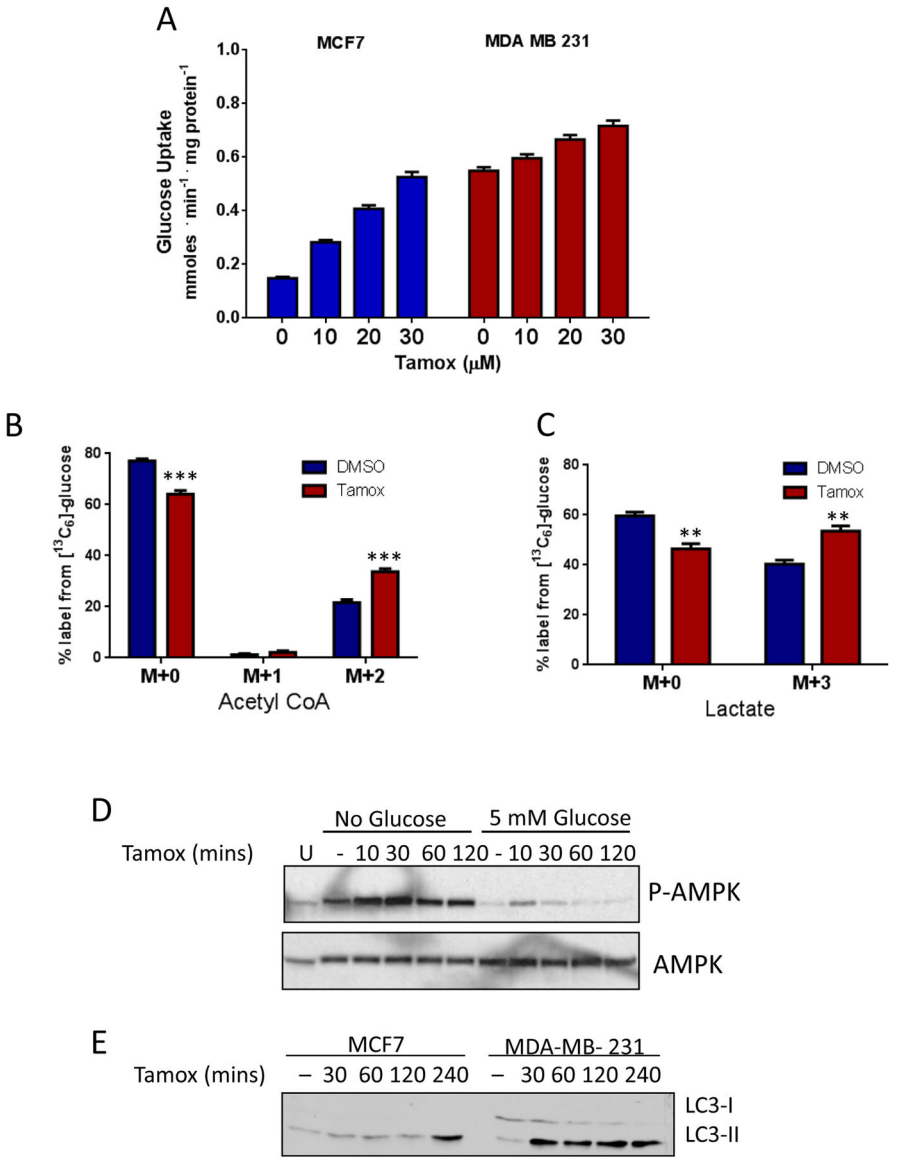

Figure 3. Tamoxifen treatment promotes glycolysis and alters fatty acid metabolism

A. Glucose uptake from media following tamoxifen treatment for 1 hour in MCF7 and MDA-MB-231 cells. Data are the average of three independent experiments ±SEM *P<0.05 **P<0.01 ***P<0.001. LC-MS/MS analysis of ^{13}C6-glucose metabolites after 30μM tamoxifen treatment for 1 hour in MDA-MB-231 cells: Mass isotopomer analysis of B. Acetyl CoA and C. Lactate. N=4, **P<0.01 ***P<0.001. D. Immunoblot analysis of phos-AMPK and total AMPK of cells treated with 20μM tamoxifen over time under glucose deprivation or 5mM glucose. E. Immunoblot analysis of LC3-I and LC3-II in BC cells after tamoxifen treatment.

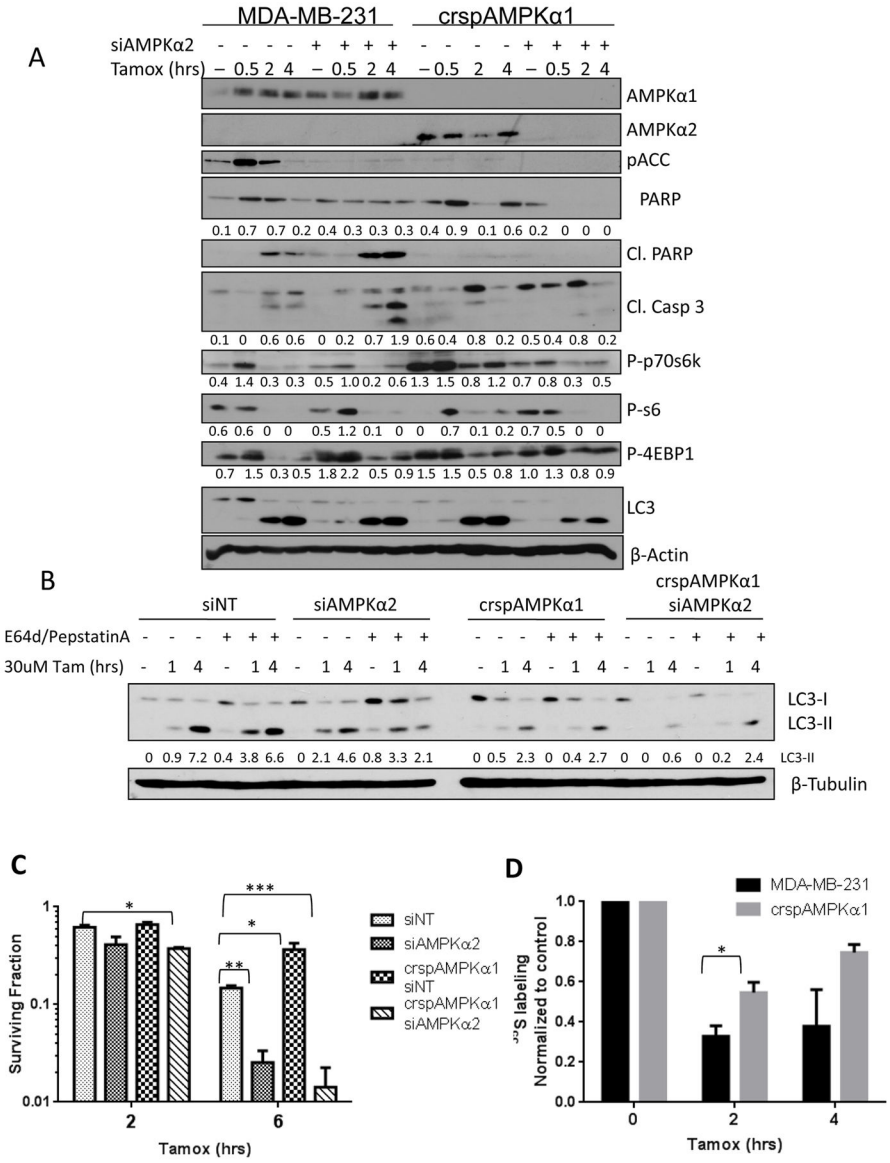

Figure 4. AMPKα1 and AMPKα2 mediate divergent effects on downstream effectors and cellular survival after tamoxifen treatment

A. Immunoblot blot of AMPK pathway activation and apoptotic markers after tamoxifen treatment. Values below blots represent pixel intensity normalized to loading control, β-Actin. B. Immunoblot of LC3-I and LC3-II flux with tamoxifen treatment as affected by AMPK status. Values represent Pixel intensity of LC3-I (top) or LC3-II (bottom) normalized to untreated control. C. Survival of AMPK knock down cells treated with 30μM tamoxifen for 4 hrs. Data are the average of four independent experiments ±SEM *P<0.05 **P<0.01 ***P<0.001C. D. Quantification of ^{35}S labeling after tamoxifen treatment in MDA231 cells and AMPK CRISPR knock out cells. Data are the average of three independent experiments ±SEM *P<0.05.

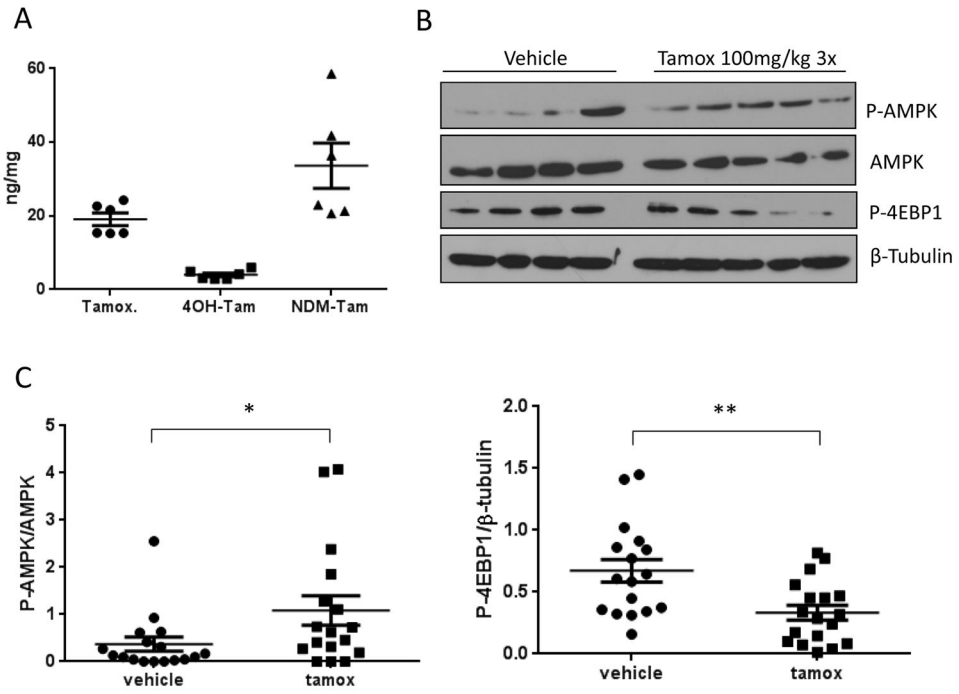

Figure 5. Activation of the AMPK pathway by tamoxifen *in vivo*

A. Tamoxifen and its metabolite levels in tumor tissue from 6 representative lysates following treatment with tamoxifen (100mg/kg) for 3 days analyzed by LC-MS/MS. B. Representative Immunoblot of AMPK pathway activation in tumor lysates. C. Densitometry analysis of signal intensity of Phos-AMPK normalized to total AMPK and Phos-4EBP1 normalized to β-Tubulin. Data is the average ±SEM of N=17 per group, *P<0.05 **P<0.01.

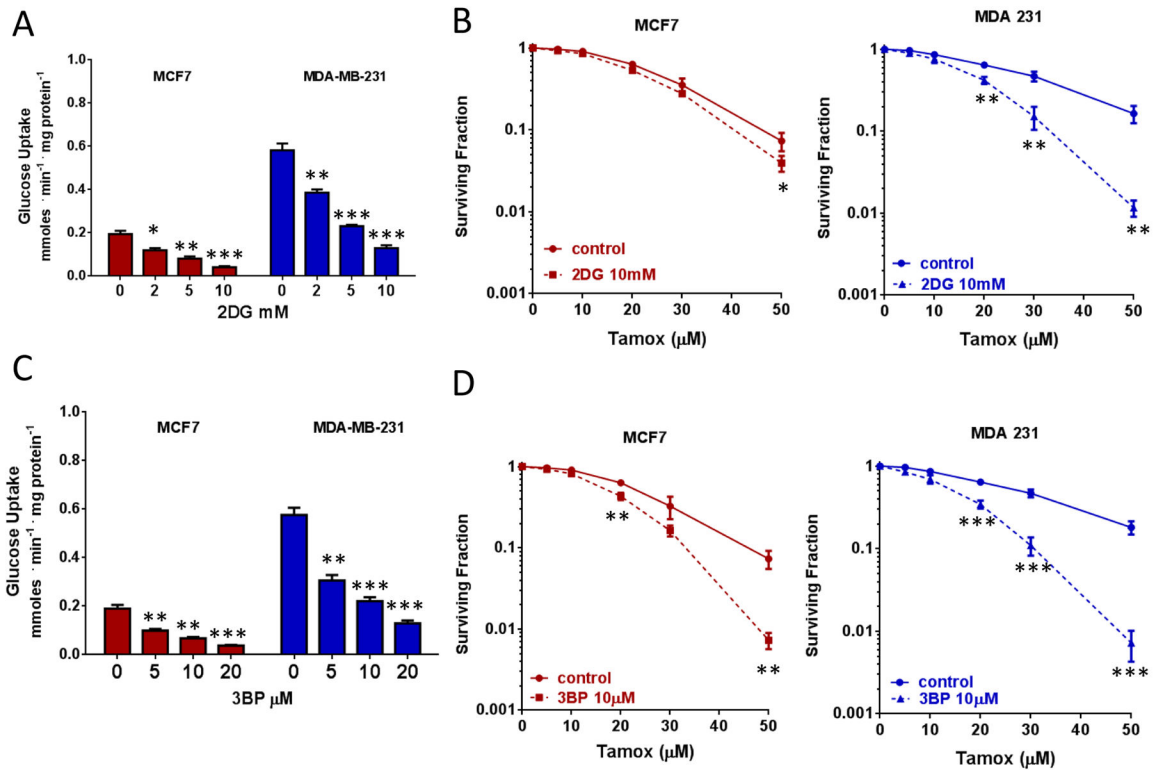

Figure 6. Tamoxifen in strategies of combined cytotoxicity

A. Glucose uptake measurements in BC cells treated with 2DG. B. Survival of BC cells treated with 2DG and tamoxifen or tamoxifen alone. C. Glucose uptake measurements in BC cells treated with 3-BP. D. Survival of BC cells treated with 3-BP and tamoxifen or tamoxifen alone. Data are the average of three independent experiments ±SEM *P<0.05 **P<0.01 ***P<0.001.

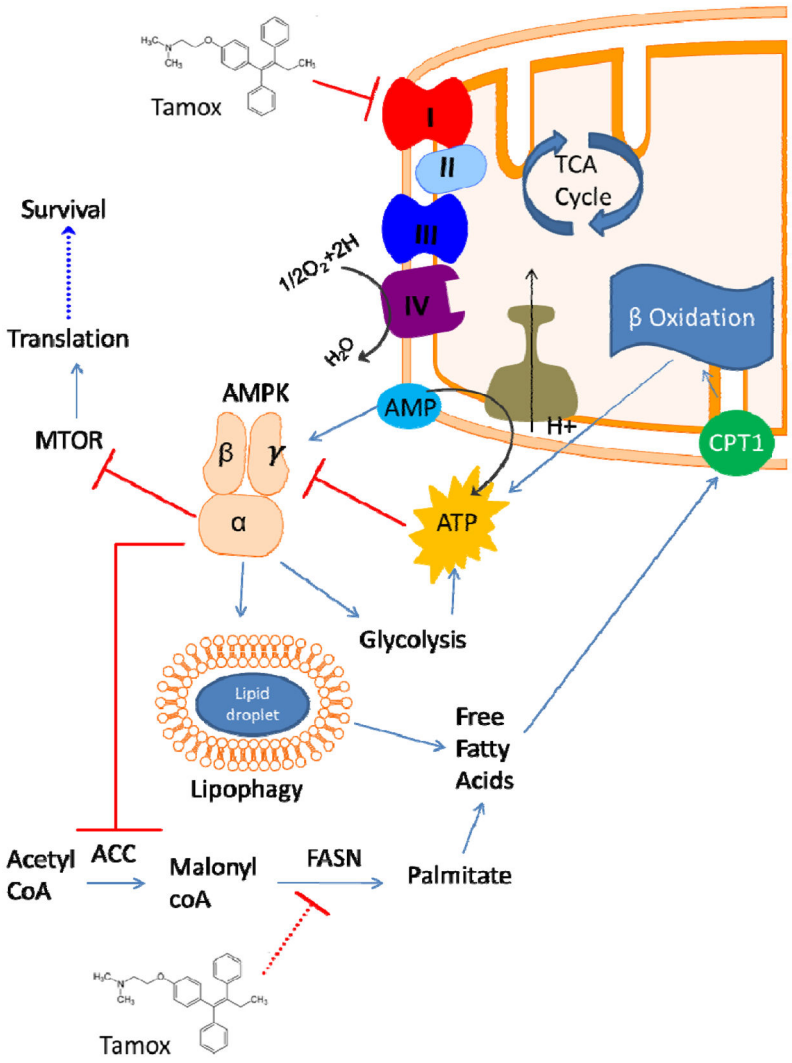

Figure 7. Model of the effects of tamoxifen on cellular metabolism and AMPK signaling

Tamoxifen directly inhibits the mitochondrial electron transport chain at complex I. This results in a decrease in consumption of O_2 by complex IV and an increase in the AMP:ATP ratio activating AMPK and promoting glycolysis and autophagy. AMPK signaling inhibits the mTOR pathway and translation resulting in cell death following tamoxifen treatment. Modulation of fatty acid metabolism may involve direct inhibitory action of tamoxifen on FASN activity.